Catal Lett (2017) 147:1252–1262
DOI 10.1007/s10562-017-2028-2

The Nature of the Isolated Gallium Active Center for Propane Dehydrogenation on Ga/SiO_2

Viktor J. Cybulskis[1] · Shankali U. Pradhan[1] · Juan J. Lovón-Quintana[1] · Adam S. Hock[2,3] · Bo Hu[2] · Guanghui Zhang[3] · W. Nicholas Delgass[1] · Fabio H. Ribeiro[1] · Jeffrey T. Miller[1,3]

Received: 3 October 2016 / Accepted: 6 March 2017 / Published online: 23 March 2017

Abstract Single-site Ga/SiO_2 catalysts exhibit up to 99% C_3H_6 selectivity at 4% propane conversion with an initial rate of 5.4×10^{-4} (mole C_3H_6) (mole Ga)$^{-1}$ s^{-1} during propane dehydrogenation (PDH) at 550 °C. Following pre-treatment in H_2 at 550 °C, only four-coordinate, Ga^{3+}–O Lewis acid sites are observed under reaction conditions. At 650 °C in H_2, an additional isolated Ga site with lower Ga–O coordination ($N_{Ga-O}<4$) is formed and leads to a 30% decrease in the initial PDH rate per total moles of Ga. The PDH rates are equivalent when normalized by the amount of surface, four-coordinate Ga^{3+}–O, regardless of catalyst pre-treatment conditions, which indicates that these isolated Ga^{3+} centers are the catalytically relevant sites.

Graphical Abstract Isolated, Lewis acidic Ga^{3+} cations present as four-coordinate Ga^{3+}–O centers exhibit up to 99% C_3H_6 selectivity during propane dehydrogenation (PDH) at 550 °C. An additional isolated Ga site with lower Ga–O coordination is formed during H_2 treatment at elevated temperatures, but is inactive for PDH and reversibly decomposes under reaction conditions.

Electronic supplementary material The online version of this article (doi:10.1007/s10562-017-2028-2) contains supplementary material, which is available to authorized users.

✉ Jeffrey T. Miller
mill1194@purdue.edu

[1] School of Chemical Engineering, Purdue University, 480 Stadium Mall Drive, West Lafayette, IN 47907, USA

[2] Department of Chemistry, Illinois Institute of Technology, 3101 S. Dearborn Street, Chicago, IL 60616, USA

[3] Chemical Sciences and Engineering Division, Argonne National Laboratory, 9700 South Cass Avenue, Argonne, IL 60439, USA

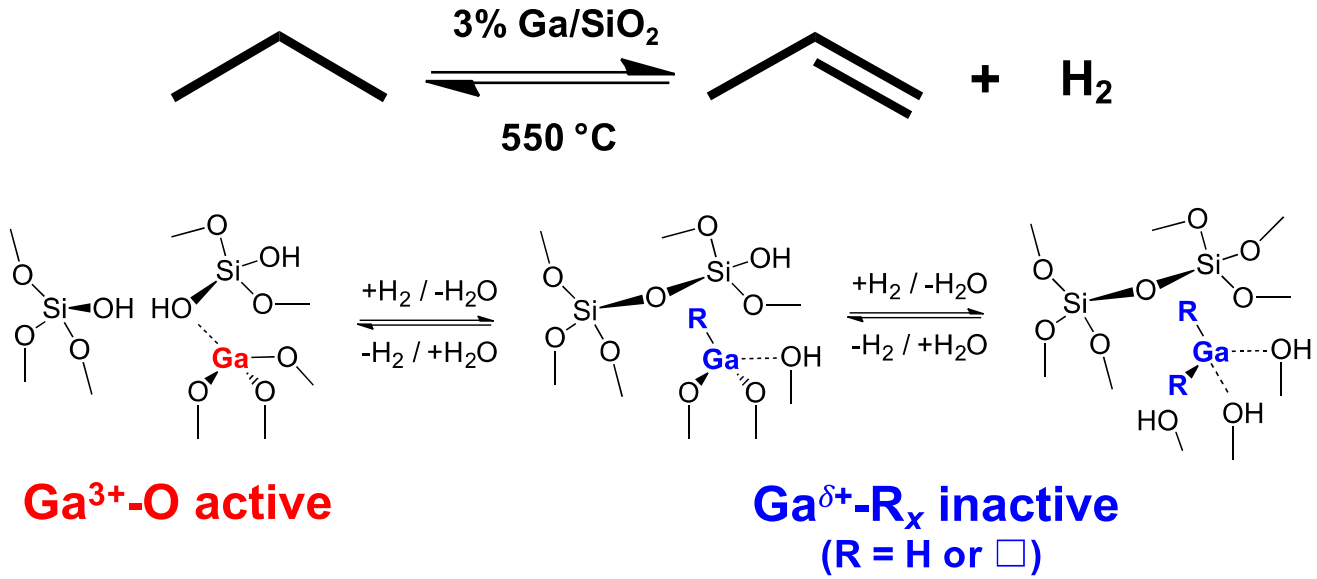

Keywords Dehydrogenation · EXAFS · NEXAFS · Heterogeneous catalysis · XPS

1 Introduction

Light alkenes, including propylene (C_3H_6), are versatile commodity chemicals that are most widely produced by steam cracking of naphtha, gas oil, and liquefied petroleum gases (LPG), such as propane (C_3H_8). In this thermally-driven process, hydrocarbons are rapidly heated in the absence of oxygen to temperatures in excess of 800 °C causing paraffinic C–C and C–H bonds to fragment and subsequently recombine in a series of free radical polymerization reactions [1, 2]. When propane is thermally cracked, a maximum C_3H_6 selectivity of approximately 50% can be achieved at low conversions ($X < 0.2$) between 725 and 750 °C [1]. At higher propane conversions, C_3H_6 selectivity decreases with the ensuing production of methane and other by-products. Additional C_3H_6 production routes include fluidized catalytic cracking (FCC) and catalytic dehydrogenation of propane (PDH). The most common PDH processes utilize PtSn/Al_2O_3 and CrO_x/Al_2O_3 catalysts, yet challenges surrounding C_3H_6 selectivity and long-term catalyst stability limit their widespread application [3, 4]. These drawbacks, coupled with recent surges in hydrocarbon production from gas-containing shale formations throughout the United States, have created new incentives to develop catalytic innovations that can selectively activate paraffinic C–H bonds and directly upgrade lower alkanes into value-added chemicals and fuels [5].

Ga- and Zn- cations have been shown to promote reactions of alkanes, such as PDH, on metal oxides [6–8]. For example, Ga-exchanged zeolites are well known to catalyze propane aromatization reactions in the commercial CYCLAR process [9, 10]. Additionally, metal oxide-supported Ga_2O_3 displays up to 85% C_3H_6 selectivity ($X = 0.2$–0.4) during PDH at 550 °C [11]. When doped with K and Pt, these metal oxide-supported Ga materials have been shown to maintain 93% C_3H_6 selectivity ($X = 0.3$) for up to 14 days [3]. It has been suggested that isolated Ga and Zn cations in metal-exchanged zeolites, such as Ga/H-ZSM-5, Zn/H-ZSM-5, and Zn/Na-ZSM-5, promote the rate of non-oxidative alkane dehydrogenation pathways by facilitating recombinative desorption of H_2 and inhibiting undesirable cracking reactions [9, 10, 12, 13]. However, the residual Brønsted acidity in these microporous aluminosilicates limits C_3H_6 selectivity by increasing the rate of propane conversion to aromatics [13]. Recent work by Schweitzer et al. [14] has demonstrated that isolated, Lewis acidic Zn^{2+} cations on inert, amorphous SiO_2 can selectively activate C–H bonds during PDH at 550 °C with greater than 90% C_3H_6 selectivity, but suffer from low turnover frequencies ($\sim 1 \times 10^{-4}$ s^{-1}). Additional SiO_2-supported, single-site transition metals, such as Cr^{3+} [15], Co^{2+} [16], and Fe^{3+} [17], have been reported to exhibit similar behavior for PDH.

Although the catalytic activity of these supported transition metal catalysts for PDH is generally accepted, the nature of their active metal sites is often a point of contention since a variety of cationic species can be observed under reaction conditions. For Ga, the proposed active species include Ga^{3+}, $[GaO]^+$, $[GaH_x]^{\delta+}$, or Ga^+ sites in

zeolites that are stabilized by the negative charge of the framework lattice [3, 4, 12, 18, 19]. A recent study by Getsoian et al. [20] has provided new evidence to suggest that features previously assigned to $Ga^{\delta+}$ in X-ray absorption near edge spectra (XANES) may also be interpreted as low-coordinate Ga^{3+}–H_x or Ga^{3+}–R_x species on Ga-impregnated zeolites and SiO_2-supported single-site Ga and that this new assignment could have important implications when considering how isolated Ga sites are able to activate paraffinic C–H bonds in lower alkanes. In the present study, we combine infrared (IR) spectroscopy of adsorbed pyridine, in situ IR spectroscopy, *operando* X-ray absorption spectroscopy (XAS), X-ray photoelectron spectroscopy (XPS), and steady-state kinetic measurements in order to identify the Ga species present on SiO_2-supported single-site Ga catalysts and determine the nature of the catalytically relevant Ga center during PDH.

2 Experimental

2.1 Catalyst Synthesis

The Ga/SiO_2 catalysts were prepared by Getsoian et al. [20] according to a pH-controlled incipient wetness impregnation (pH-IWI) method. Approximately 20 g of commercially available high-purity SiO_2 (Davisil Grade 646, 300 m^2 g^{-1}) was impregnated with an aqueous solution of 3 g $Ga(NO_3)_3{\cdot}xH_2O$ and 3 g citric acid in 15 ml of deionized water to obtain ~3 wt% Ga loading. The pH of the solution was adjusted to 11 with 4 ml of concentrated NH_4OH. The pre-catalyst was dried overnight in an oven at 110 °C and then calcined in air at 550 °C for 3 h. The final Ga loading was measured at Galbraith Laboratories by using inductively coupled plasma atomic emission spectroscopy (ICP-AES) and determined to be 2.64 wt%.

2.2 Kinetic Measurements

PDH kinetic measurements were performed in a vertical, quartz, plug flow reactor (PFR, Wilmad Lab Glass, 10 mm O.D. thin wall) at 1 bar. A K-type thermocouple (3.2 mm O.D.) for temperature indication was placed inside of a quartz sheath and inserted through a well in the reactor and into the center of the catalyst bed at the midpoint to measure the reaction temperature inside of the bed. A furnace (ATS 3210, 870 W) connected to a temperature controller (Eurotherm 2408) was used to supply heat to the reactor and maintain the reaction at the desired temperature.

The reaction gas mixture was supplied by four, parallel mass flow controllers to a manifold that mixes the gases prior to entering the reactor. In order to determine the contribution of gas-phase thermal cracking reactions to the overall PDH rate, a gas mixture consisting of 5% C_3H_8 (Matheson, 99.5%), 10% Ar (Matheson, 99.999%), which was used as an internal standard, and balance He (Matheson, 99.999%) was introduced into an empty, clean reactor at 60 ml min^{-1} total flow while the temperature was ramped from RT to 550 °C at 10 °C min^{-1}. The total flow rate was confirmed at the reactor outlet by use of a bubble flow meter. The reactor effluent was analyzed by using an Agilent 6890 GC equipped with a thermal conductivity detector (TCD) as well as a flame ionization detector (FID). A Carboxen 1000 GC column connected to the TCD was used to separate the permanent gases in the reactor effluent gas mixture, while a GS-GASPRO capillary column connected to the FID was used to separate the hydrocarbon components. It was verified that the rate of gas-phase thermal cracking in the empty reactor tube was below detection limits at 550 °C.

Approximately 300 mg of sieved (150 μm < d_p < 250 μm) Ga/SiO_2 was loaded into the reactor on top of a support bed that consisted of quartz chips (~1/8″) followed by quartz wool. The catalyst was pre-treated in He (Matheson, 99.999%) at 75 ml min^{-1} for 15 min at RT. The temperature was: (i) ramped from RT to 100 °C at 10 °C min^{-1}, (ii) held at 100 °C for 15 min, (iii) ramped to 550 °C at 10 °C min^{-1}, and (iv) then held at 550 °C for 2 h before switching to the PDH reaction mixture (5% C_3H_8, 10% Ar, bal. He).

Subsequent pre-treatment studies included: (a) exposing the fresh Ga/SiO_2 catalyst to H_2 (Praxair, 99.999%) for 1 h at 550 °C, and (b) exposing the fresh Ga/SiO_2 catalyst to H_2 for 1 h at 650 °C. During these pre-treatments, pure H_2 was passed across the catalyst at RT for 15 min at 25 ml min^{-1}. The temperature was ramped from RT to either 550 or 650 °C at 10 °C min^{-1} and then held at the desired temperature for 1 h. Following the H_2 treatment, the reactor was flushed with He at 50 ml min^{-1} for 15 min. The catalyst was then stabilized in the PDH reaction mixture at 550 °C for 13 h to ensure that the steady-state propane conversion remained below 10%. Details regarding the calculation of propane conversion and product selectivity can be found in Sect. 1 of the supplementary material.

2.3 Transmission Infrared Spectroscopy

Fourier transform IR spectroscopy was used to examine the surface features associated with Ga/SiO_2. Between 55 and 80 mg of catalyst was pressed into a 20 mm-diameter self-supporting wafer and loaded into a quartz transmission IR gas cell whose design has been described elsewhere [21]. The assembled IR cell was placed inside of an

IR spectrometer (Nicolet 4700), evacuated to ~10^{-2} Torr, and then heated to 150 °C for 1 h to remove residual moisture from the sample wafer and quartz cell. The sample was treated in 10% Ar and balance He (50 ml min^1) and IR background spectra were collected for Ga/SiO_2 at 150, 450, 500, 550, and 650 °C.

Pyridine (Alfa Aesar, >99%) was purified by three sets of freeze–thaw–degas cycles and then introduced into the IR cell from a custom glass manifold in order to identify the presence of Lewis and Brønsted acid sites. The IR cell was then evacuated to ~10^2 Torr to remove residual physisorbed pyridine from the catalyst surface. IR spectra were collected at 2 cm^{-1} resolution by averaging 64 scans between 400 and 4000 cm^{-1} relative to the sample wafer background reference under vacuum. In situ IR experiments were performed under H_2 flow (25 ml min^{-1}) on a fresh Ga/SiO_2 wafer following pre-treatment in 10% Ar and balance He (50 ml min^1) from RT to 650 °C. The in situ IR spectra were collected relative to the sample wafer background reference under flow of inert.

2.4 *Operando* X-ray Absorption Spectroscopy

Gallium *K* edge (10.375 keV) *operando* XAS experiments were performed in transmission mode at the Materials Research Collaborative Access Team (MRCAT) insertion device (10-ID) beam line at the Advanced Photon Source (APS) within Argonne National Laboratory. Ga/SiO_2 samples were pre-treated under pure H_2 at 550 or 650 °C for 1 h, cooled to room temperature under He, and then heated to 550 °C under the PDH feed mixture (5% C_3H_8, 10% Ar, bal. He) in a vertical, quartz tube reactor (Wilmad Lab Glass, 5 mm O.D. thin wall, 10 mm O.D. ends) at a total flow rate of 30 ml min^{-1}. The 5 mm O.D. reactor was chosen for the *operando* XAS measurements in order to minimize the absorption path length and attenuation of the X-ray beam by the SiO_2 support while maximizing the signal-to-noise ratio. Approximately 150 mg of catalyst was loaded into the reactor in order to maintain the same weight-hourly space velocity (WHSV) of 12,000 ml g_{cat}^{-1} h^{-1} as the 10 mm O.D. laboratory PFR. The catalyst bed was held in place by a bed of quartz wool and quartz chips (~1/8″). A vertical, cylindrical furnace (ATS 3210, 870 W) with a radial bore-through hole (~6 mm diameter) was used to supply heat to the reactor while enabling simultaneous X-ray transmission through the catalyst bed. Kinetic analysis was performed by using the same Agilent 6890 GC equipped with Carboxen 1000 and GS-GASPRO columns as previously described.

XANES spectra were obtained by using standard methods and were energy calibrated by comparing the standard edge position to the simultaneously obtained edge position of a gallium (III) acetylacetonate reference compound (10.377 keV) [12, 19, 20, 22], denoted as $Ga(AcAc)_3$. The Ga edge energy was determined based on the position of the maximum of the first peak in the first derivative of the XANES region. Phase shifts and backscattering amplitudes for the extended X-ray absorption fine structure (EXAFS) were determined for Ga–O scattering based on the experimentally obtained $Ga(AcAc)_3$ spectra ($N_{Ga-O}=6$, $R_{Ga-O}=1.94$ Å). X-ray absorption spectra were analyzed with WinXAS v. 3.1 software [23]. The values for the amplitude reduction factor, S_0^2, and Debye–Waller factor (DWF), $\Delta\sigma^2$, were determined for the first Ga–O scattering shell of the $Ga(AcAc)_3$ reference by performing a least squares fit in *R*-space of the k^2-weighted Fourier transform.

2.5 X-ray Photoelectron Spectroscopy

XPS was performed by using a Kratos Axis Ultra DLD spectrometer equipped with a monochromatic Al *Kα* source (1486.6 eV), a hemispherical electron analyzer, and a charge neutralization system. The spectrometer was operated at ~10^{-9} Torr and 75 W with 14.7 kV applied across the anode. XPS spectra were collected in constant pass energy mode at 20 eV.

The Ga/SiO_2 samples were treated in an atmospheric pressure reaction cell under pure H_2 flow at either 550 or 650 °C for 1 h. The catalysts were then transferred to the XPS chamber without exposure to air where both survey and high resolution scans were obtained for the Ga 3*d*, Ga 2*p*, Si 2*p*, O 2*s*, O 1*s*, and C 1*s* peaks. XPS spectra were curve-fit by using CasaXPS (version 2.3.15) software. The binding energies for each spectrum were energy calibrated to the Si 2*p* peak at 103.4 eV [24, 25]. Each peak was fit by using a 30–70 Gaussian–Lorentzian curve shape with a Shirley background. Optimization of the band position, area, and full width at half-maximum (FWHM) was performed through Levenberg–Marquardt iterations by minimizing the root mean square (RMS) error.

3 Results

3.1 Kinetics of PDH on Single-Site Ga/SiO_2

In addition to certifying the absence of gas-phase thermal cracking and dehydrogenation reactions for the empty PFR at 550 °C, the SiO_2 support (Davisil Grade 646) was examined for PDH between 570 and 630 °C with 5% C_3H_8, 10% Ar (internal standard), and balance He as shown by the Arrhenius plot in Figure S1. The measured apparent activation energy for the Ga-free SiO_2 support was 253 ± 17 kJ $mole^{-1}$ and C_3H_6 formation was below detectable limits at 550 °C. For the 2.64 wt% Ga/SiO_2 catalyst, the measured apparent activation energy during PDH between 530 and 570 °C was 79 ± 5 kJ $mole^{-1}$. The C_3H_8 conversion ranged

from 4 to 8% under these conditions, which is below the equilibrium conversion of 32% at 550 °C [26, 27] as shown in Figure S2 and ensures that the reported PDH rates are equivalent to the forward reaction rate. These results show that the contribution of gas-phase and SiO_2-induced dehydrogenation reactions are negligible at 550 °C; thus, confirming that the Ga sites are catalytic. IR detection of adsorbed pyridine revealed that SiO_2-supported Ga is Lewis acidic as indicated by the sharp bands at 1455, 1410, and 1610 cm^{-1}[28, 29] in Figure S4. The absence of a band at 1540 cm^{-1} due to pyridinium ion [30, 31], as indicated by the vertical dashed line, confirmed that no Brønsted acid (H^+) sites strong enough to deprotonate pyridine were present on Ga/SiO_2.

The 2.64 wt% Ga/SiO_2 catalysts used in this study were stabilized in the PDH reaction gas mixture (5% C_3H_8, 10% Ar, bal. He) at 550 °C after the following pre-treatment conditions: (i) under 100% He flow at 550 °C for 2 h, (ii) under 100% H_2 flow at 550 °C for 1 h, and (iii) under 100% H_2 flow at 650 °C for 1 h. Previous studies have suggested that reduced Ga, $[GaH_x]^{\delta+}$, or Ga^{3+}–H_x species are formed during H_2 pre-treatment at elevated temperatures ($T > 500$ °C) and are only stable under reaction conditions [12, 18–20].

The steady-state PDH rates for the 12 h stabilization period on each 2.64 wt% Ga/SiO_2 sample at different pre-treatment conditions are shown in Fig. 1. As indicated by the similar deactivation curves for the He-550 °C (white ○) and H_2-550 °C (blue ■) pre-treated samples, both samples exhibited initial PDH rates of 5–5.5 × 10^{-4} (mole C_3H_6) (mole Ga)$^{-1}$ s^{-1} that stabilized to ~3 × 10^{-4} (mole C_3H_6) (mole Ga)$^{-1}$ s^{-1}, thus indicating that a similar Ga active site was present under these conditions. For the H_2-650 °C (red ▲) pre-treated sample, however; the initial PDH rate of 3.7 × 10^{-4} (mole C_3H_6) (mole Ga)$^{-1}$ s^{-1} was approximately 30% lower than the initial rates for the He-550 °C and H_2-550 °C pre-treated samples and deactivated to ~3 × 10^{-4} (mole C_3H_6) (mole Ga)$^{-1}$ s^{-1}. The decrease in initial PDH rate per total moles of Ga following H_2 treatment at 650 °C implies either a loss in the total number of Ga active sites, or that the surface chemistry of these Ga sites was altered upon exposure to H_2 at high temperatures.

Examination of in situ IR spectra obtained under flow of H_2 revealed the presence of surface silanol (SiOH) groups that were gradually dehydroxylated between 450 and 650 °C as indicated by the decrease of the ν(O–H) band at 3740 cm^{-1} (Fig. S4a). Simultaneously, a band appeared at 3670 cm^1 that is assigned to the ν(O–H) stretch of either Ga–OH or Si–O(H)–Ga [32, 33]. This band that was formed upon H_2 treatment at elevated temperatures in conjunction with the ν(Ga–H) band at 2035 cm^{-1} (Fig. S4b) and has been observed by others [32, 34–37], is likely due to heterolytic dissociation of H_2 at the Ga site. The intensity of this Ga–H feature increased under flow of H_2 up to

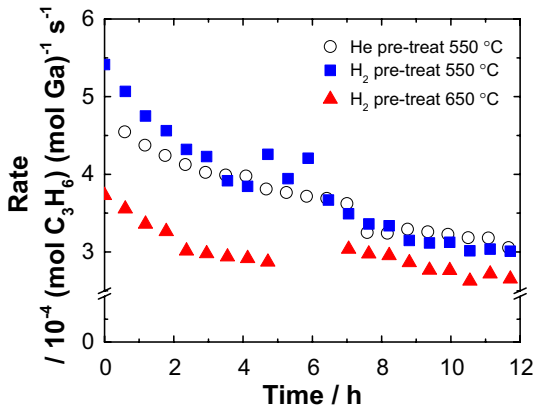

Fig. 1 Comparison of PDH stabilization in 5% C_3H_8, 10% Ar, and balance He at 550 °C for 2.64% wt% Ga/SiO_2 pre-treated in: He at 550 °C (*circle*), H_2 at 550 °C (*filled square*), and H_2 at 650 °C (*filled triangle*)

650 °C, where an additional band at 1980 cm^{-1} was formed. Pulham et al. [38] have attributed the ν(Ga–H) stretch at 1976 cm^{-1} to the two terminal hydrogen vibrations (H–Ga–H) in digallane model compounds. This assignment of a second hydrogen coordinated to the isolated Ga site is consistent with the model proposed by Getsoian et al. [20] where two different Ga–H species at 10.371 and 10.373 keV were identified by ΔXANES on Ga/SiO_2 after H_2 pre-treatment at 650 °C.

3.2 *Operando* XAS during PDH on Single-Site Ga/SiO_2

To examine the working state of the Ga active center for the 2.64 wt% Ga/SiO_2 catalysts, transmission XAS spectra were obtained during PDH at 550 °C under the same conditions as in the laboratory PFR. Experiments were performed at the Ga *K* edge (10.375 keV) for Ga/SiO_2 to measure the $1s \rightarrow 4p$ transition. XANES spectra were used to identify the chemical state and valence of Ga along with adsorbed surface species while EXAFS provided information on the Ga coordination (*N*) as well as the type of nearest neighbors and bond distances (*R*).

The as-is 2.64 wt% Ga/SiO_2 catalyst was compared against β-Ga_2O_3, which is a mixture of tetrahedral and octahedral phases ($N_{Ga-O} = 5$), and $Ga(AcAc)_3$ ($N_{Ga-O} = 6$) at room temperature in air. As indicated by the EXAFS in Figure S5, Ga/SiO_2, β-Ga_2O_3, and $Ga(AcAc)_3$ exhibited Ga–O coordination in the first scattering shell at ~1.8 Å. The higher shells for β-Ga_2O_3 indicated Ga–O–Ga coordination, which was absent on Ga/SiO_2 and confirms that the Ga species in 2.64 wt% Ga/SiO_2 were isolated as single cations. This Ga/SiO_2 sample was then pre-treated in He at 550 °C and examined during PDH (5% C_3H_8, 10% Ar, bal. He) at 550 °C. The agreement between the PDH rates

obtained in the laboratory PFR and those in the *operando* setup, as shown in Figure S6, confirmed that, by maintaining the same WHSV of 12,000 ml g_{cat}^{-1} h^{-1}, the smaller diameter *operando* XAS reactor (5 mm O.D.) was able to replicate the kinetics obtained from the laboratory PFR (10 mm O.D.).

Following pre-treatment in H_2 at 550 °C for 1 h, the 2.64 wt% Ga/SiO_2 catalyst was examined under PDH (5% C_3H_8, 10% Ar, bal. He) at 550 °C for 1.5 h while XAS spectra at the Ga *K* edge were simultaneously collected. The XANES spectra exhibited an absorption maximum at approximately 10.377 keV (Fig. 2a), which is indicative of Ga^{3+} and has been observed by others [12, 19, 20, 22]. This Ga^{3+} feature remained constant during the 1.5 h PDH experiment on the H_2-550 °C pre-treated Ga/SiO_2 sample. Additionally, the isolated first shell EXAFS revealed that the isolated Ga^{3+} cations were bound to 4 oxygen atoms, as compared to the $Ga(AcAc)_3$ reference compound, and remained stable throughout the 1.5 h reaction as four-coordinate species with Ga–O bonds at 1.80 ± 0.01 Å. (Fig. 2b). These four-coordinate Ga^{3+}–O sites exhibited an initial PDH rate of 5.4×10^{-4} (mole C_3H_8) (mole Ga)$^{-1}$ s^{-1} with 99.2% C_3H_6 selectivity at 4% C_3H_8 conversion. The EXAFS fitting parameters and kinetic data for this sample are listed in the top half of Table 1.

After pre-treatment in H_2 at 650 °C for 1 h, an additional XANES feature for Ga/SiO_2 was observed approximately 4 eV lower than the Ga^{3+} absorbance maximum at 10.377 keV as shown in Fig. 3 (magenta line). This lower energy XANES feature has been observed by others [12, 18, 19] following H_2 pre-treatment of Ga/H-ZSM-5 at elevated temperatures and was previously assigned to a reduced Ga^+, GaO^+, or $[GaH_x]^{\delta+}$. However, by preparing a series of Ga^{3+} compounds of varying Ga-ligand coordination, Getsoian et al. [20] recently demonstrated that this shift in the XANES edge energy can also be explained by the influence of the ligand on the Ga^{3+} center rather than simply a reduction in Ga oxidation state. A comparison of the XANES in Figure S7 for synthetically-prepared $Ga(CH_2SiMe_3)_3$ (dashed line), a molecular model compound containing a Ga^{3+} cation with three Ga–C bonds, and its heterogeneous analog, $Ga(CH_2SiMe_3)_3/SiO_2$ (blue line) with the H_2-650 °C pre-treated Ga/SiO_2 catalyst (magenta line) reveals that the observed decrease in XANES energy for Ga/SiO_2 is consistent with the Ga^{3+}–R_x assignment for the reference materials [20].

When compared to the Ga^{3+} XANES for the H_2-550 °C pre-treated Ga/SiO_2 sample (black line) in Fig. 3, it is evident that the H_2-650 °C pre-treated Ga/SiO_2 sample contained some fraction of four-coordinate Ga^{3+}–O as indicated by the absorption peak maximum at 10.377 keV. Additionally, it is worth noting that the low energy XANES feature at 10.373 keV remained stable not only in H_2 at 650 °C (red line), but also in He at 550 °C (blue line) and He at RT (magenta line). The stability of this secondary Ga species is contradictory to what has been observed by Meitzner et al. [12] for reduced Ga on Ga/H-ZSM-5, which was present only under reaction conditions. Individual EXAFS fitting parameters for the H_2-650 °C pre-treated Ga/SiO_2 sample can be found in Table S1.

After XANES spectra were obtained at RT in He, the H_2-650 °C pre-treated Ga/SiO_2 catalyst was heated to 550 °C and examined during PDH (5% C_3H_8, 10% Ar, bal. He) for 1.5 h while XAS spectra at the Ga *K* edge were simultaneously collected. In contrast to the H_2-550 °C pre-treated Ga/SiO_2 catalyst, which remained as

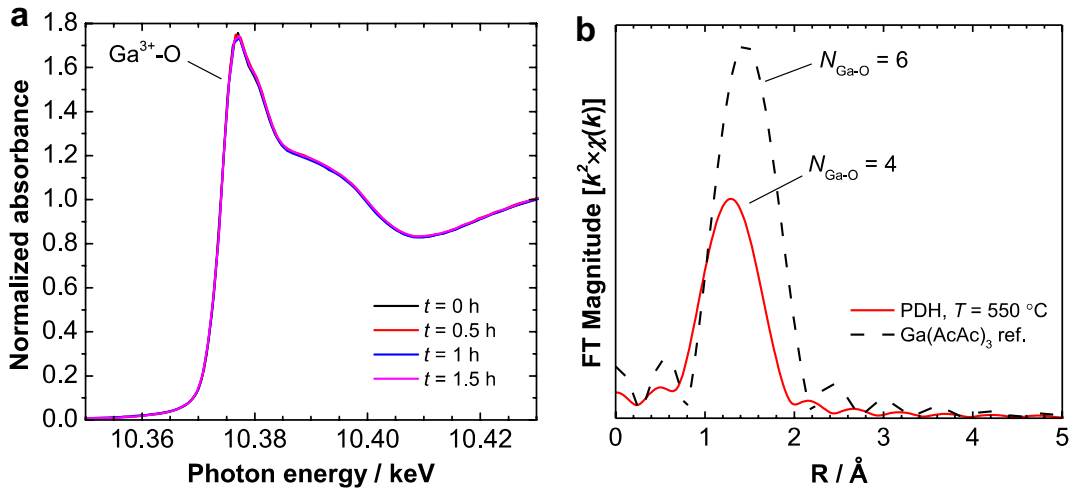

Fig. 2 *Operando* Ga K edge **a** XANES and **b** EXAFS of first scattering shell. Obtained during PDH at 550 °C for 2.64 wt% Ga/SiO_2 after H_2 pre-treatment at 550 °C

Table 1 EXAFS fittings of first scattering shell for 2.64 wt. % Ga/SiO_2 measured during PDH after H_2 pre-treatment at 550 and 650 °C

Sample	PDH rate[a] /10^{-4} (mole C_3H_6) (mole Ga)$^{-1}$ s^{-1}	$S_{C_3H_6}$	t/h	N_{Ga-O}	R_{Ga-O}/Å	σ^2
2.64 wt% Ga/SiO_2 550 °C H_2 pre-treat	5.4	99.2	0	4.1 ± 0.4	1.80 ± 0.01	0.006
	5.1	99.0	0.5	4.1 ± 0.4	1.80 ± 0.01	
	4.8	98.9	1	4.0 ± 0.4	1.80 ± 0.01	
	4.6	98.7	1.5	4.1 ± 0.4	1.80 ± 0.01	
2.64 wt% Ga/SiO_2 650 °C H_2 pre-treat	3.7	97.4	0	2.6 ± 0.3	1.80 ± 0.01	0.006
	3.5	97.8	0.5	2.7 ± 0.3	1.79 ± 0.01	
	3.3	97.5	1	3.0 ± 0.3	1.80 ± 0.01	
	–	–	1.5	3.2 ± 0.3	1.80 ± 0.01	

[a]Measured at 550 °C in 5% C_3H_8, 10% Ar, and bal. He

[b]C_3H_6 selectivity at 4% C_3H_8 conversion

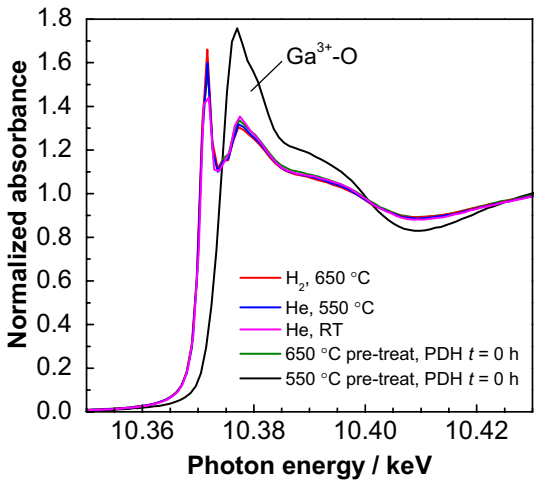

Fig. 3 Comparison of Ga *K* edge XANES for 2.64 wt% Ga/SiO_2 in various atmospheres after H_2 pre-treatment at 650 °C with 2.64 wt% Ga/SiO_2 in PDH mixture at 550 °C after H_2 pre-treatment at 550 °C (*solid black line*)

four-coordinate Ga^{3+} throughout the reaction, the intensity of the low energy XANES feature at 10.373 keV for the H_2-650 °C pre-treated Ga/SiO_2 sample gradually decreased with time on stream as the Ga^{3+} feature at 10.377 keV gradually increased (Fig. 4a). Furthermore, the isolated first shell EXAFS in Fig. 4b shows that N_{Ga-O} increased with time during PDH at 550 °C. The EXAFS fitting parameters and kinetic data in the bottom half of Table 1 show that the H_2-650 °C pre-treated Ga/SiO_2 catalyst exhibited an average Ga–O coordination of 2.6 ± 0.3 with a bond distance of 1.80 ± 0.01 Å at $t = 0$ h and increased to 3.2 ± 0.3 by $t = 1.5$ h. This Ga^{3+} center, with a lower Ga–O coordination ($N_{Ga-O} < 4$) than the H_2-550 °C pre-treated sample, had an initial PDH rate of 3.7×10^{-4} (mole C_3H_6) (mole Ga)$^{-1}$ s^{-1} with 97.4% C_3H_6 selectivity at ~4% C_3H_8 conversion.

3.3 XPS for Single-Site Ga/SiO_2

The 2.64 wt% Ga/SiO_2 catalyst was treated in a reaction cell at atmospheric pressure per the same procedures used for the kinetic analysis and *operando* XAS study: (i) under 100% H_2 flow at 550 °C for 1 h, and (ii) under 100% H_2 flow at 650 °C for 1 h. Following pre-treatment, the catalyst was transferred to the XPS chamber (~10^{-9} Torr) without exposure to air in order to obtain spectra for the Ga 3*d*, Ga 2*p*, Si 2*p*, O 2*s*, O 1*s*, and C 1*s* peaks. All spectra were energy calibrated to the Si 2*p* peak at 103.4 eV [24, 25]. The Ga $2p_{3/2}$ peak was chosen for curve fitting due to the better signal-to-noise ratio compared to the Ga $3d_{5/2}$ peak.

Deconvoluted Ga $2p_{3/2}$ XPS spectra for the H_2-550 °C and H_2-650 °C pre-treated Ga/SiO_2 catalysts are shown in Fig. 5a, b, respectively. Both Ga $2p_{3/2}$ bands exhibit two features: a dominant peak at 1119.0 eV that is assigned to Ga^{3+} [39–42], and a lower binding energy shoulder at 1117.7 eV that has been assigned by others as either Ga^+ [43–45] or Ga^{2+} [32]. However, based on the Ga^{3+}-H_x/Ga^{3+}-R_x XANES assignment by Getsoian et al. [20] for Ga-impregnated zeolites and Ga/SiO_2 after H_2 pre-treatment, it is possible that this low energy peak at 1117.7 eV, which lies between Ga^{3+} (1119.0 eV) [39–42] and Ga^0 (1117.0 eV) [41], may also be explained by the reduced Ga–O coordination at the Ga^{3+} site as a result of Ga^{3+}–H_x formation. The gradual replacement of O ligands on four-coordinate Ga^{3+} by less electronegative, σ-donating H results in increased electron density on the isolated Ga center and lowers the binding energy of the Ga $2p_{3/2}$ electron, which is consistent with the additional shoulder at 1117.7 eV that is observed on Ga/SiO_2 after H_2 pre-treatment.

The relative surface concentrations of the Ga^{3+} (i.e., Ga^{3+}–O) and secondary Ga species at 1119V and 1117.7 eV, respectively, are shown in Table 2 as atomic percentages for the H_2-550 °C and H_2-650 °C pre-treated Ga/SiO_2 samples. The elemental compositions were

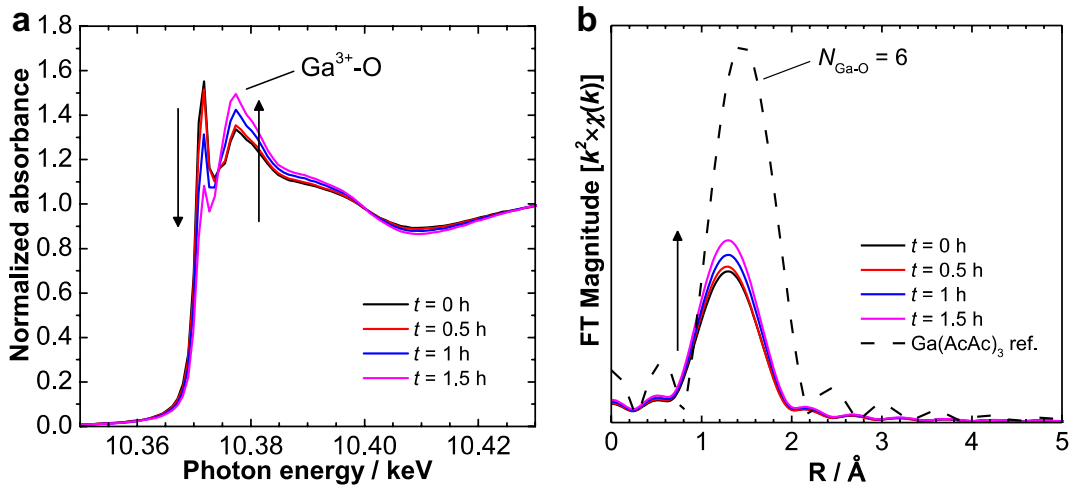

Fig. 4 *Operando* Ga *K* edge **a** XANES and **b** EXAFS of first scattering shell. Obtained during PDH at 550 °C for 2.64 wt% Ga/SiO_2 after H_2 pre-treatment at 650 °C

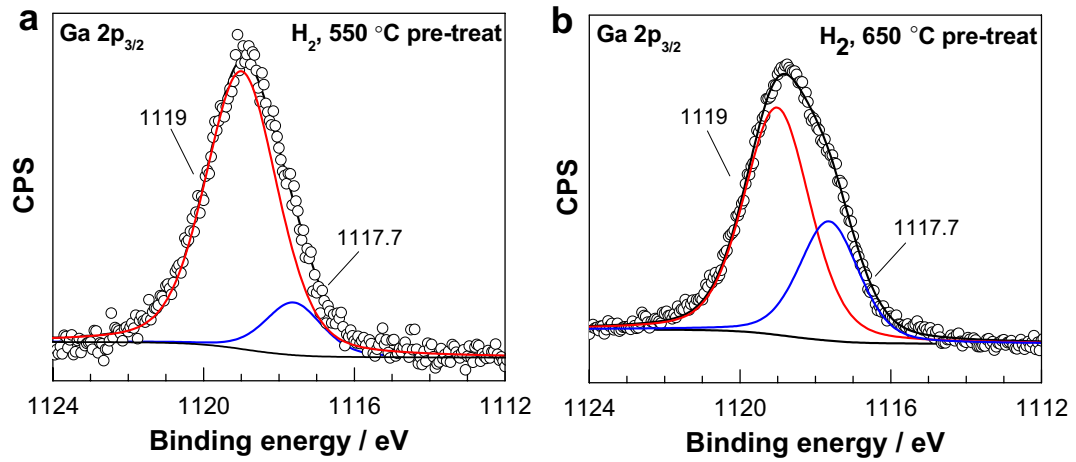

Fig. 5 Ga $2p_{3/2}$ XPS spectra for: **a** 2.64 wt% Ga/SiO_2 after H_2 pre-treatment at 550 °C, and **b** 2.64 wt% Ga/SiO_2 after H_2 pre-treatment at 650 °C

determined by curve-fitting the Ga 2*p*, Si 2*p*, O 1*s*, and C 1*s* peaks per the method described in Sect. 2.4. As indicated in Table 2, the Ga/SiO_2 sample that was pre-treated in H_2 at 550 °C contained only a small fraction of low-coordinate Ga while nearly 40% of the surface Ga on the H_2-650 °C pre-treated sample was present as this second type of isolated Ga species. However, when normalized by the fraction of four-coordinate Ga^{3+}–O on the surface, rather than the total moles of Ga, the initial PDH rates for both Ga/SiO_2 samples were equivalent at ~6.4×10^{-4} (mole C_3H_6) (mole $Ga^{3+})^{-1}$ s^{-1}. The implications of these findings are discussed further below.

4 Discussion

The SiO_2-supported single-site Ga catalysts in this study exhibited high (up to 99%) C_3H_6 selectivity during PDH at 550 °C ($X=0.04$), which is congruent with reports for other Zn- and Ga-containing zeolites and metal oxides [3, 9, 12–14]. The initial dehydrogenation rate of 5.4×10^4 (mole C_3H_6) (mole Ga)$^{-1}$ s^{-1} at 550 °C for Ga/SiO_2 is comparable to values reported under similar conditions for gallium oxide-based dehydrogenation catalysts (~5×10^{-4} (mole olefin) (mole Ga)$^{-1}$ s^{-1}) [46, 47], commercial CrO_x/Al_2O_3 catalysts (~7×10^{-4} (mole olefin) (mole Cr)$^{-1}$ s^{-1}) [48], and a Cr/SiO_2 catalyst prepared with well-defined Cr sites (~8×10^{-4} (mole C_3H_6) (mole Cr)$^{-1}$ s^{-1}) [15]. For the present work, the combination of kinetics and *operando* XAS

Table 2 Quantifcation of Ga $2p_{3/2}$ XPS spectra and normalization of PDH rates by surface Ga^{3+} for samples treated in H_2 at 550 and 650 °C

Sample	Ga^{3+} −1119.0 eV /atomic %	Ga−1117.7 eV /atomic %	PDH rate[a] /10^{-4} (mole C_3H_6) (mole Ga)$^{-1}$ s^{-1}	Normalized rate[b] /10^{-4} (mole C_3H_6) (mole Ga^{3+})$^{-1}$ s^{-1}
2.64 wt% Ga/SiO_2 550 °C H_2 pre-treat	1.1	0.2	5.4	6.4
2.64 wt% Ga/SiO_2 650 °C H_2 pre-treat	1.0	0.7	3.7	6.3

[a]Initial rate measured at 550 °C in 5% C_3H_8, 10% Ar, and bal. He

[b]Normalized by contribution of Ga^{3+} at 1119.0 eV

revealed that the active Ga in Ga/SiO_2 was present as isolated, Lewis acidic Ga^{3+} cations rather than an extra-crystalline Ga_2O_3 phase. One potential structure for this active site consists of an isolated Ga^{3+} cation bound to three Si–O bonds with the Ga center coordinated to an additional oxygen on a neighboring Si–O bond through the lone electron pair to maintain charge neutrality in the absence of residual Brønsted acid sites. Additional SiO_2-supported, single-site transition metal catalysts such as Zn^{2+} [14], Co^{2+} [16], and Fe^{2+} [17] have been examined for PDH with XAS. Zn/SiO_2 contains four-coordinate Zn^{2+}–O, which can form lower coordinate Zn–O species during reaction while Co/SiO_2 and Fe/SiO_2 remain and four-coordinate Co^{2+}–O and three-coordinate Fe^{2+}–O isolated species, respectively. For the case of Ga/SiO_2, there are likely multiple Si–O configurations on the surface of the amorphous SiO_2 support that can coordinate with various Ga^{3+} ions via covalent bonding. While the detailed structure of Ga/SiO_2 at the atomic level is not yet known, the nature of the isolated Ga species, which is a function of the catalyst pre-treatment conditions, has importance consequences on kinetic performance.

It has been proposed that framework Ga sites within zeolites facilitate the rate-determining H^+/H^- recombination and H_2 desorption step during alkane dehydrogenation by stabilizing hydride surface species [12, 49–51]. For Ga/SiO_2 and Ga-containing zeolites, these hydride surface species have been observed [20, 32, 34, 35] after H_2 treatment at elevated temperatures ($T > 550$ °C) and have been shown by Getsoian et al. [20] to produce shifts in the Ga *K* edge XANES similar to reduced gallium, Ga^+, and Ga_2O species [3, 4, 12, 18, 19, 52]. In situ IR experiments for Ga/SiO_2 catalysts prepared under similar conditions in the current study revealed that at least one or more Ga–H surface features are formed in the presence of H_2 between 550 °C and 650 °C. The initial PDH rate per total moles of Ga was ~30% lower at 550 °C on the Ga/SiO_2 catalyst that was pre-treated in H_2 at 650 °C and contained a larger fraction of Ga–H compared to Ga/SiO_2 pre-treated in H_2 at 550 °C. Analysis of the Ga/SiO_2 surface by XPS supports *operando* XAS results, which indicate that at least two types of Ga surface species are present following H_2 pre-treatment. The lower binding energy shoulder for the Ga $2p_{3/2}$ electron, which lies between peaks assigned to Ga^{3+} and Ga^0, is traditionally attributed to either Ga^+ or Ga^{2+} [32, 43–45]. However, the shift in binding energy from Ga^{3+} at 1119.0 eV to 1117.7 eV after exposure to H_2 at high temperatures may also be explained by the formation of Ga^{3+}–H_x sites with reduced Ga–O coordination. The replacement of oxygen ligands on Ga by σ-donating H species will modify the Lewis acidity of these sites as increased electron density is placed at the Ga center.

Although XANES and XPS features consistent with Ga^{3+}–H_x and IR signatures for Ga–H surface species were observed under similar conditions for Ga/SiO_2 in the current study, the possibility of a reduction in the Ga oxidation state cannot be ruled out entirely as reduced Ga species would also give rise to energy shifts for both XANES and XPS. Thus, based on these findings, we tentatively assign this second isolated Ga site to low-coordinate $Ga^{\delta+}$-R species, where R may correspond to one or more H ligands coordinated to Ga^{3+}, or a vacancy (□) in the case of reduced Ga center. While shown to be present only under reaction conditions for Ga/H-ZSM-5 catalysts [12]. The $Ga^{\delta+}$-R site on Ga/SiO_2 was stable in H_2 and He atmospheres from RT to 650 °C, but reversibly decomposed to Ga^{3+}–O in the presence of C_3H_8 at 550 °C. However, as shown in Fig. 1, the PDH rate for the H_2-650 °C pre-treated sample (red triangles) did not increase upon loss of the $Ga^{\delta+}$–R site due to simultaneous deactivation that occurred via carbon deposition (i.e., coking) on the catalyst surface. A comparison between the three pre-treatment conditions in Fig. 1 reveals that deactivation proceeded through a similar mechanism on each catalyst during the 12 h stabilization period.

The fraction of $Ga^{\delta+}$–R present on the H_2-650 °C pre-treated Ga/SiO_2 sample, as determined by XPS, indicates that up to 40% of the surface Ga was present as this secondary, isolated Ga site while the H_2-550 °C pre-treated Ga/SiO_2 sample contained less than 15% $Ga^{\delta+}$–R. Thus, the

PDH rates for these catalysts were nearly identical when normalized by the fraction of surface Ga^{3+}–O rather than total moles of Ga. These findings indicate that only four-coordinate, single-site Ga^{3+}–O species are active for PDH on Ga/SiO_2. At elevated pre-treatment temperatures in H_2, a less stable, inactive $Ga^{\delta+}$–R species is formed. The difference in PDH rates per Ga between the H_2-550 °C and H_2-650 °C pre-treated Ga/SiO_2 catalysts can be reconciled by the relative surface coverages of $Ga^{\delta+}$–R for these samples.

The multiple Ga surface species present during PDH along with facile decomposition of $Ga^{\delta+}$–R and concomitant catalyst deactivation hinders one's ability to deconvolute the dynamic surface processes that occur in order to identify the true active sites. These experimental challenges highlight the importance of *operando* characterization techniques where the catalyst performance can be directly correlated to surface features or structural changes during the reaction in order to avoid misleading conclusions. While there has been much debate in the literature over the precise assignment of low energy Ga XANES features assigned to either Ga^{3+}–H_x or $Ga^{\delta+}$ species, where $0<\delta<3$ [3, 4, 12, 18–20, 52], its identity is of secondary importance for this work. The combination of steady-state kinetics and *operando* XAS confirms that this observed $Ga^{\delta+}$–R surface intermediate is a spectator species during PDH on Ga/SiO_2. Therefore, the mechanism to selectively activate C–H bonds over single-site Ga/SiO_2 is not redox in nature, nor does the presence of gallium hydrides or $Ga^{\delta+}$ sites appear to be essential for hydrogen recombination. Indeed, various computational and experimental studies on Ga-exchanged zeolites have shown that non-redox pathways, such as sigma-bond metathesis or heterolytic bond cleavage, can occur at Ga^{3+} sites [20, 51, 53, 54]. Similar findings were reported for PDH on CrO_x/Al_2O_3 and Cr^{3+}/SiO_2 catalysts, which suggested that Cr^{3+}–O surface species can activate C_3H_8 via sigma-bond metathesis by generating a Cr-alkyl intermediate that subsequently undergoes β-hydride elimination to form C_3H_6 [15, 55, 56]. The well-defined Cr^{3+} sites investigated by Conely et al. [15] exhibited similar PDH rates and deactivation behavior compared to the isolated Ga^{3+}–O sites in the current study.

For H_2 recombination on Ga/H-ZSM-5 during propane aromatization, Gonzales et al. [51] have shown with DFT and H_2/D_2 exchange that ZGaO sites can readily adsorb H_2, but that reduction of the Ga site would not proceed beyond ZGa(H)(OH). Furthermore, the barriers for H_2 release from either the ZGaO or $ZGa(H)_2$ sites in Ga/H-ZSM-5 are unfavorable [51, 53, 54], which suggests that a different type of site, such as a distant Brønsted site [57], is required to support H_2 removal in the presence of alkanes. Frash and van Santen [58] have previously proposed carbenium- and alkyl- activation pathways during ethane dehydrogenation on Ga/H-ZSM-5 to support Ga–C coordination observed upon C–H bond activation, but show that the large barrier for alkene desorption from the Ga–R_x sites will limit turnover frequencies. Our examination of single-site Ga/SiO_2 supports the observation that carbon deposition from alkene dehydrogenation at the Ga center will lead to catalyst deactivation. These findings evince a potential dichotomy between C_3H_6 selectivity and intrinsic turnover frequencies that is inherent to supported Ga catalysts for PDH. The absence of Brønsted acidity on single-site Ga/SiO_2 enables the isolated, Ga^{3+} Lewis centers to achieve up to 99% C_3H_6 selectivity, but at the cost of low (~6×10^{-4} (mole C_3H_6) (mole $Ga^{3+})^{-1}$ s^{-1}) dehydrogenation rates in comparison to Pt-containing catalysts (~10^{-1} (mole olefin) (mole Pt)$^{-1}$ s^{-1}) [4]. However, if residual Brønsted sites are required for facile H_2 release, then C_3H_6 selectivity may diminish due to subsequent oligomerization and cyclization reactions.

5 Conclusions

Isolated, Lewis acidic Ga^{3+} sites dispersed on amorphous SiO_2 are catalytic for PDH at 550 °C and can activate hydrocarbon C–H bonds with up to 99% selectivity through a non-redox pathway. The four-coordinate Ga^{3+} sites initially present on Ga/SiO_2 with 4 Ga–O bonds can be converted to a second type of isolated Ga site with reduced Ga–O coordination during H_2 pre-treatment at elevated temperatures, which produce energy shifts in XAS and XPS spectra that are often assigned to $Ga^{\delta+}$ sites, where $0<\delta<3$, but are also consistent with Ga^{3+}–R surface species. While these spectroscopically observable $Ga^{\delta+}$–R sites remain stable in inert and H_2 atmospheres from RT to 550 °C, they reversibly decompose in the presence of C_3H_6 under reaction conditions to regenerate the Ga^{3+}–O site. The subsequent decrease in PDH rate is a result of coke formation at the Ga center. Although catalysts containing $Ga^{\delta+}$–R surface species exhibit lower initial PDH rates per total moles of Ga compared to samples with pure, four-coordinate Ga^{3+}–O sites, the rates are equivalent when normalized by the fraction of Ga^{3+} present on the surface despite the method of catalyst pre-treatment. Thus, the isolated, four-coordinate Ga^{3+}–O centers are shown to be the catalytically relevant sites on Ga/SiO_2 while $Ga^{\delta+}$–R species are identified as spectators.

Acknowledgements Support for this research was provided by Qatar National Research Fund No. 13121024. Funding for A.S.H., B.H., G.Z., and J.T.M. was provided by the U.S. Department of Energy, Division of Chemical Sciences, Geosciences, and Biosciences, under contract DE-AC0-06CH1137. Use of the Advanced Photon Source is supported by the U.S. Department of Energy, Office of Science, and Office of Basic Energy Sciences, under

Contract DE-AC02-06CH11357. MRCAT operations are supported by the Department of Energy and the MRCAT member institutions. The authors would like to thank Andrew "Bean" Getsoian for assistance with analysis of Ga *K* edge XANES spectra. Also, the authors acknowledge Dmitry Zemlyanov in the Birck Nanotechnology Center at Purdue University for performing the XPS characterization.

References

1. Buekens AG, Froment GF (1968) Ind Eng Chem Res 7:435–447
2. Burdick DL, Leffler WL (2001) Petrochemicals in nontechnical language, Pennwell Books, Tulsa, pp. 65–85
3. Sattler, JJHB, Gonzalez-Jimenez ID, Luo L, Stears BA, Malek A, Barton DG, Kilos BA, Kaminsky MP, Verhoeven T, Koers EJ, Baldus M, Weckhuysen BM (2014) Angew Chem Int Ed 53:9251–9256
4. Sattler, JJHB, Ruiz-Martinez J, Santillan-Jimenez E, Weckhuysen BM (2014) Chem Rev 114:10613–10653
5. Siirola JJ (2014) AIChE J 60:810–819
6. Kitagawa H, Sendoda Y, Ono Y (1986) J Catal 101:12–18
7. Mowry JR, Anderson RF, Johnson JA (1985) Oil Gas J 83:128–131
8. Mole T, Anderson JR, Creer G (1985) Appl Catal 17:141–154
9. Biscardi JA, Iglesia E (1996) Catal Today 31:207–231
10. Bhan A, Nicholas Delgass, W. (2008) Catal Rev 50:19–151
11. Xu BJ, Zheng B, Hua WM, Yue YH, Gao Z (2006) J Catal 239:470–477
12. Meitzner GD, Iglesia E, Baumgartner JE, Huang ES (1993) J Catal 140:209–225
13. Biscardi JA, Iglesia E (1999) Phys Chem Chem Phys 1:5753–5759
14. Schweitzer NM, Hu B, Das U, Kim H, Greeley J, Curtiss LA, Stair PC, Miller JT, Hock AS (2014) ACS Catal 4:1091–1098
15. Conley MP, Delley MF, Nunez-Zarur F, Comas-Vives A, Coperet C (2015) Inorg Chem 54:5065–5078
16. Hu B, Getsoian A, Schweitzer NM, Das U, Kim H, Niklas J, Poluektov O, Curtiss LA, Stair PC, Miller JT, Hock AS (2015) J Catal 322:24–37
17. Hu B, Schweitzer NM, Zhang GH, Kraft SJ, Childers DJ, Lanci MP, Miller JT, Hock AS (2015) ACS Catal 5:3494–3503
18. Rane N, Overweg, AR, Kazansky VB, van Santen RA, Hensen EJM (2006) J Catal 239:478–485
19. Hensen EJM, Garcia-Sanchez M, Rane N, Magusin P, Liu PH, Chao KJ, van Santen RA (2005) Catal Lett 101:79–85
20. Getsoian AB, Das U, Bunquin JC, Zhang G, Gallagher JR, Hu B, Cheah S, Schaidle JA, Ruddy DA, Hensley JE, Krause TR, Curtiss LA, Miller JT, Hock AS (2016) Catal Sci Technol 6:6339–6353
21. Cybulskis VJ, Harris JW, Zvinevich Y, Ribeiro FH, Gounder R (2016) Rev Sci Instrum 87:1031011–1031018
22. Nishi K, Shimizu K, Takamatsu M, Yoshida H, Satsuma A, Tanaka T, Yoshida S, Hattori T (1998) J Phys Chem B 102:10190–10195
23. Ressler T (1998) J Synchrotron Radiat 5:118–122
24. Chao SS, Takagi Y, Lucovsky G, Pai P, Custer RC, Tyler JE, Keem JE (1986) Appl Surf Sci 26:575–583
25. Gross T, Ramm M, Sonntag H, Unger W, Weijers HM, Adem EH (1992) Surf Interface Anal 18:59–64
26. Gomez-Quero S, Tsoufis T, Rudolf P, Makkee M, Kapteijn F, Rothenberg G (2013) Catal Sci Technol 3:962–971
27. Stull DR, Westburn EF, Sinke GC (1969) The chemical thermodynamics of organic compounds, Wiley, New York, pp. 198–329
28. Tamura M, Shimizu K, Satsuma A (2012) Appl Catal A: Gen 433:135–145
29. Vimont A, Lavalley JC, Sahibed-Dine A, Arean CO, Delgado MR, Daturi M (2005) J Phys Chem B 109:9656–9664
30. Emeis CA (1993) J Catal 141:347–354
31. Parrillo DJ, Adamo AT, Kokotailo GT, Gorte RJ (1990) Appl Catal 67:107–118
32. Collins SE, Baltanas MA, Fierro JLG, Bonivardi AL (2002) J Catal 211:252–264
33. Sulikowski B, Olejniczak Z, Corberan VC (1996) J Phys Chem 100:10323–10330
34. Kazansky VB, Subbotina IR, van Santen RA, Hensen EJM (2005) J Catal 233:351–358
35. Kazansky VB, Subbotina IR, van Santen RA, Hensen EJM (2004) J Catal 227:263–269
36. Collins SE, Baltanas MA, Bonivardi AL (2005) Langmuir 21:962–970
37. Vecchietti J, Baltanás MA, Gervais C, Collins SE, Blanco G, Matz O, Calatayud M, Bonivardi A (2017) J Catal 345:258–269
38. Pulham CR, Downs AJ, Goode MJ, Rankin DWH, Robertson HE (1991) J Am Chem Soc 113:5149–5162
39. Kanazirev V, Price GL, Tyuliev G (1992) Zeolites 12:846–850
40. Serykh AI, Amiridis MD (2009) Surf Sci 603:2037–2041
41. Cossu G, Ingo GM, Mattogno G, Padeletti G, Proietti GM (1992) Appl Surf Sci 56–8:81–88
42. Breeze PA, Hartnagel HL, Sherwood PMA (1980) J Electrochem Soc 127:454–461
43. Carli R, Bianchi CL (1994) Appl Surf Sci 74:99–102
44. Carli R, Bianchi CL, Giannantonio R, Ragaini V (1993) J Mol Catal 83:379–389
45. Scharmann F, Cherkashinin G, Breternitz V, Knedlik C, Hartung G, Weber T, Schaefer JA (2004) Surf Interface Anal 36:981–985
46. Nesterenko NS, Ponomoreva OA, Yuschenko VV, Ivanova II, Testa F, Di Renzo F, Fajula F (2003) Appl Catal A: Gen 254:261–272
47. Saito M, Watanabe S, Takahara I, Inaba M, Murata K (2003) Catal Lett 89:213–217
48. Shee D, Sayari A (2010) Appl Catal A 389:155–164
49. Meriaudeau P, Naccache C (1990) J Mol Catal 59:L31–L36
50. Iglesia E, Baumgartner JE, Price GL (1992) J Catal 134:549–571
51. Gonzales NO, Chakraborty AK, Bell AT (1999) Top Catal 9:207–213
52. Price GL, Kanazirev V (1990) J Catal 126:267–278
53. Joshi YV, Thomson KT (2007) J Catal 246:249–265
54. Joshi YV, Thomson KT (2005) Catal Today 105:106–121
55. Olsbye U, Virnovskaia A, Prytz O, Tinnemans SJ, Weckhuysen BM (2005) Catal Lett 103:143–148
56. Weckhuysen BM, Schoonheydt RA (1999) Catal Today 51:223–232
57. Le Van Mao R, Dufresne L (1989) Appl Catal 52:1–18
58. Frash MV, van Santen RA (2000) J Phys Chem A 104:2468–2475